Budker Institute of Nuclear Physics

SIBERIAN SYNCHROTRON RADIATION CENTRE

S.V. Chernov, B.P. Tolochko, S.G. Nikitenko

"IN SITU" INVESTIGATION OF THE INITIAL STAGE OF THE SYNTHESIS OF HIGH-TEMPERATURE PHASE OF NICKEL MOLYBDATE

BUDKER INP 96-12

NOVOSIBIRSK

1996

"IN SITU" INVESTIGATION OF THE INITIAL STAGE OF THE SYNTHESIS OF HIGH-TEMPERATURE PHASE OF NICKEL MOLYBDATE

[1]S.V.Chernov, [1]B.P.Tolochko, [2]S.G.Nikitenko
Budker Institute Of Nuclear Physics
630090, Novosibirsk, Russia

Abstract

By means of analysis of fluorescence spectra close to and far off the K-edge of nickel (XANES and EXAFS methods) during the synthesis of nickel molybdate by the reaction $NiO+\alpha\text{-}MoO_3 \rightarrow \beta\text{-}NiOMoO_4$, an unknown phase was observed which can be related to a product with low atomic nickel content. Nickel coordination with oxygen atoms is in this phase substantially different from octahedral. This signifies that there are several stage of the synthesis. At the initial stage of this synthesis , the traditional formation of the layer of final product, $\beta\text{-}NiOMoO_4$, and its smooth growing for the next time do not take place but an intermidiate phase is formed. The possible phase are offered and analysed.

[1] Institute of Solid State Chemistry, 630090 Novosibirsk, Russian Federation
[2]Boreskov Institute of Catalysis, 630090 Novosibirsk, Russian Federation
e-mail: chernov@inp.nsk.su
tolochko@inp.nsk.su
nix@sunsr.inp.nsk.su

INTRODUCTION

The properties and the formation of high-temperature nickel molybdate phase, β-$NiOMoO_4$, obtained in the deposition of the powder NiO+α-MoO_3 mixture and its further heating, have been repeatedly studied [1-4]. It was claimed in [3,4] that the structure of β-$NiOMoO_4$ is isomorphous to that of α-$MnMoO_4$. According to [5], the synthesis mechanism was considered in the similar systems (MeO+α-MoO_3 , where Me = Ni, Co, Cd) as the formation of the layer of final product, β-$NiOMoO_4$ in the case under consideration, at the contact points of the crystallites of the two initial compounds, and further growth of this layer due to the diffusion of the atoms of initial compounds through it and their interactions. But no experimental data to confirm this mechanism have been obtained by now. Therefore, in the present work we have attempted to study the initial stage of β-$NiOMoO_4$ synthesis and to determine the structure of the initially formed product by experimental means. Two methods of X-ray absorption spectra analysis [6-10] have been used for this purpose, one of them (x-absorption near edge structure, or XANES) involving the absorption near the K-edge of nickel during the synthesis, and another (expanded x-absorption fine structure, or EXAFS) far off the K-absorption edge of nickel.

XANES spectrum is known to give the information on the nearest surroundings of the absorbing atom. It is essentially dependent on the chemical nature of atoms and on the geometry, mainly in the first coordination sphere. EXAFS analysis allows to determine the distance from the absorbing atom to the neighbouring atoms of several nearest coordination spheres by separating the oscillating component of the spectrum (fine structure) in the range 50 - 1000 eV (3 - 6 A^{-1}) beyond the absorption edge and carrying out its Fourier transformation to the **R**-space. EXAFS analysis gives little or no information on the topology of the construction. Having united these two methods, we tried to study the synthesis kinetics of the high-temperature phase of nickel molybdate. Along with the experimental data, we used also the results of XANES spectra simulation for various types of nickel surrounding by oxygen atoms. Besides, the peaks in the **R**-space of EXAFS spectrum were reconstructed for the assumed arrangement of oxygen and molybdenum atoms in the vicinity of the absorbing nickel atom.

The results of our study suggest that the consept of the mechanism of β-$NiOMoO_4$ synthesis mentioned above is questionable. It is obvious that the surrounding of nickel is not octahedral at the initial stage of synthesis, as it would be in the case of nickel molybdate, but its structure is probably low-symmetry packing in the nearest coordination sphere.

The next section deals with experimental data obtained when treating the fluorescence XANES and EXAFS spectra of X-ray absorption by nickel at the K-edge in the mixture NiO+α-MoO_3. Theoretical modelling of the experimental data and the proposals concerning possible construction of the nearest surroundings of nickel are discussed in the consequent chapters.

.

TREATMENT OF EXPERIMENTAL XANES AND EXAFS SPECTRA

A powder mixture NiO+α-MoO_3 pressed in a massive copper cell was used as a sample in the experiment. The cell was placed on the surface of the heating element. The relation NiO : α-MoO_3 in the sample was equal to 0.1:1. A sample of pure NiO was used for comparison. XANES and EXAFS spectra were obtained at the EXAFS station of the storing ring of the VEPP-3 at the Siberian Synchrotrone Radiation Centre of the Institute of Nuclear Physics of Siberian Branch of Academy of Science [11]. The electron beam energy was 2 GeV and the current was 100 mA. A double monoblock crystal Si(111) monochromator was used for X-ray monochromatization. The spectra were registered at the K-edge of nickel with a ~1 eV step. Since the measurements were

carried out according to the fluorescence technique, the contribution from higher harmonic components of monochromatic radiation had practically no impact on the shape of the spectra. The orientation of the sample and the detector was chosen so as to meet two demands: (i) to minimize self-absorption of the fluorescence in the sample and in the air, otherwise this effect could distort the shape of the spectrum; and (ii) to decrease the scattered radiation falling at the detector. Electroluminescent gas counter operating in the current regime was used as a detector [11]. It was placed perpendicular to the polarization plane of synchrotron radiation for the purpose of decreasing the effect of scattered emission on the quality of the spectra.

The selection of normalized oscillating part of the EXAFS spectrum, $\chi(k)$, followed by the Fourier transformation from $k^3\chi(k)$ was carried out using a standard packet of programs UWXAFS 3.0 [12,13]. A reference calculation of $\chi(k)$ was carried out for the absorption spectrum at the K-edge of nickel in a well-known structure (NiO) in order to determine the energy of the K-edge of nickel. Fourier transformation was carried out in the range 2.5 - 12 $(A)^{-1}$. A strict relationship [14,15] is known to exist between the positions of radial distribution peaks of the Fourier transform (FT) and the distance from the absorbing atom to its nearest neighbours. But there is no exact coincidence of real distance values with those determined with FT. Quantum chemical calculations are needed for more precise identification.

Fig.1 represents FT for pure NiO at room temperature and at 600^0C. One can clearly see the peaks related to the coordination spheres of oxygen and nickel atoms in the lattice of NaCl type. This type is characterized by large coordination numbers, therefore, the amplitudes of the peaks are rather high and clearly distinguished from each other up to long distances (~5A). The discrepancy between the curves is caused by the increase of thermal oscillations of the lattice, as well as by small thermal strains in the sample. FT obtained for the sample containing the mixture NiO+α-MoO_3

heated for 2 h at 600^0C (Fig.2) exhibit different behaviour. Beside the first small false peak, only two essentially intensive peaks are observed in the region up to 4 A. The second peak which is located at the distance of 1.7 A occupies the same position as the first oxygen peak at Fig.1 and gives the typical distance of Ni - O, ~2A, after the correction is made. The second peak located at 2.8A cannot be explained on the basis of the structure of β-$NiMoO_4$. The structure of this compound is isomorphous to the structures of α-$MnMoO_4$ and α-$MgMoO_4$. Molybdenum atoms are located inside the tetrahedrons composed of oxygen atoms, while nickel atoms, similar to NiO, occupy the positions inside the distorted oxygen octahedrons [16]. Ni-O distance is 2.1 - 2.25 A for

the first oxygen sphere and Ni-Ni distance is 3.35 and 3.48 A , accordingly. The smallest Ni-Mo distances in this structure are larger, 3.55 - 3.80 A. The calculation of the correction to FT distances for Ni-Ni from the known distances in NiO structure (Fig.1) gives ~0.2 A. Since the value of this shift is nearly independent of the character of a chemical compound, we inevitably come to the conclusion that it is impossible to explain the third peak at Fig.2 neither by nickel coordination in the structure of β-$NiOMoO_4$ nor by the coordination characteristic of NiO structure.

This conclusion is more vividly seen when treating XANES spectra at the K-edge of Ni recorded for one and the same sample when heating the mixture (0.1)NiO+(1.0)α-MoO_3 to 600^0C and keeping it for 2 h at this temperature (Fig.2). Diffractometry data evidence to the complete disappearance of the reflections of NiO as a result of heating. This means that the interaction of NiO with MoO_3 has been completed. Consequently, the residual MoO_3 is present in the mixture along with the product of the interaction of NiO with MoO_3. If β-$NiOMoO_4$ were obtained as a result of the interaction, the nearest surroundings of nickel would not be changed. Nickel is located within oxygen octahedrons both in NiO and β-$NiOMoO_4$. But Fig.2 exhibits the substantial change of the shape of the spectrum beyond the K-edge of nickel which depicts the substantial change of the geometry of the nearest coordination sphere of nickel during the reaction. The decrease of the intensity of the peak beyond the K-edge of nickel, which appears as a result of heating (Fig.2), can be due to the lowering of the symmetry of the nearest surroundings of nickel in the new product. This statement is confirmed below by numerical modelling.

The analysis of XANES and EXAFS spectra given above makes us sure that we observe the formation of new intermediate phase which is the product of NiO+a-MoO_3 interaction at the early stage of the synthesis. This product is characterized by low concentration of Ni during the interaction with a-MoO_3.

THEORETICAL MODEL

A) EXAFS analysis

On the basis of the experimental data reported above, we made an attempt to analyze the idea of NiO dissolution during heating in a possible structural modification of molybdenum oxide. It is known that heating of MoO_3 in a vacuum silicone tube above 800^0C followed by cooling in water always leads to the formation of nonhomogeneous product consisting of at least three phases, MoO_3, MoO_2, and Mo_4O_{11} [17]. The concentration of MoO_2 is sharply decreased at slower

cooling, while that of Mo_4O_{11} increases. From the other hand, the structure of γ-MoO_4O_{11} is the most porous among other molybdenum oxides. This can be clearly seen from Table 1 [18].

Table 1. Unit cell volume divided by the number of oxigen atoms per cell (V/N) [19,20].

Molibdenum oxide	V/N
MoO_2	16.4
γ-Mo_4O_{11}(orthorhombic)	20.5
η-Mo_4O_{11}(monoclinic)	20.3
$Mo_{17}O_{47}$	17.8
Mo_5O_{14}	18.6
Mo_8O_{23}	19.1
Mo_9O_{26}(monoclinic)	18.7
Mo9O_{26}(triclinic)	17.1
α-MoO_3	16.9
β-MoO_3	17.6

It should be noted that α-MoO_3 is highly volatile at 600^0C and above. The reaction rate increased with increasing the temperature above 600^0C but the reaction became impossible at 690^0C due to the rapid sublimation of MoO_3 which was deposited on the walls of the cell in the form of single crystal fine flakes. The elevated mobility of α-MoO_3 can possibly help the formation of the seats of another phase, namely Mo_4O_{11}, on the surface rather than in the volume. Orthorhombic modification, or γ-phase, is stable in the temperature range involved in the experiment (600 - 650^0C). The structure of this phase was determined in [21] and also in [18]. Three of the four molybdenum atoms occupy the centres of oxygen octahedrons, while the fourth is in the centre of oxygen tetrahedron. Octahedrons are connected with each other only through the top points and form two-dimensional layers. The layers are connected with each other through the tops of oxygen tetrahedrons. These connections are characterized by the presence of wide empty pentagonal channels which are stretched continuously along the crystal axis **c**. These channels may be responsible for the high reaction rate [22]. Empty cells (pores) between oxygen octahedrons are smaller, so the diffusion along them is hampered, perhaps being unable to provide the observed reaction rate. It should be noted that pentagonal channels with the space sufficient for NiO

molecules account for only ~1/4 of the total volume of the pores in the elementary cell, since every three oxygen octahedrons in γ-Mo_4O_{11} are accompanied by only one tetrahedron in the neighbouhood of which the pentagonal channel is formed. The observed new phase with low NiO concentration can be due to the initial filling of the spacious pentagonal channels.

Starting from this assumption, Monte-Carlo calculations have been carried out [23] in order to find possible optimal positions of NiO molecule in the fixed g-Mo_4O_{11} structure. The dual potential of interaction for nickel and oxygen atoms was used in the search for the position characterized by the minimal energy of the interaction of nickel with oxygen and with the fixed g-Mo_4O_{11} lattice. The calculations were carried out without taking into account the effect of temperature on the lattice. The dual potential was chosen in the following form:

$$V(r) = Z_i Z_j / r + (|Z_i Z_j| / r\,(n+1)) \cdot ((d_i + d_j)/ r)^n,$$

where i (or j) is the number of the ion, Z_i is the ion charge, r is the distance between two ions, d_i is the ion radius, and n is a parameter characterizing the rigidity of ion cores pushing apart. This form has proved itself being useful in the calculation of tetrahedron coordination in SiO_2 structure [24,25]. In our case, the parameters were chosen so as to represent the correct values for Ni-O distance (~2.0 A) in NiO lattice (of the NaCl type) and the bond energy of the ions in the lattice, taking the reaction $Ni^{2+}+O^{2-} \rightarrow$ NiO (~42.6 eV) [26,27]. The radius values for molybdenum ions were chosen according to the dimensions of their first coordination sphere. Thus, the chosen values were: Z_0= -2, Z_{ni}= +2, Z_{Mo1}= +6 (for molybdenum ions in octahedrons), Z_{mo2}= +4 (for molybdenum ions in tetrahedrons), d_0=1.3 A, d_{Ni}=0.7 A, d_{Mo1}=0.60, d_{Mo2}=0.40, n=13.

It was determined by the numerical modelling that nickel ions are really located in the pentagonal channels , slightly shifted towards the edges of the tetrahedrons, approximately in the middle of the space between these edges. Oxygen ion is located in the free inter-oxygen space in the angle adjacent to the two pentagonal channels and at the distance of ~2A from the nickel ion. Using the values from the obtained model for the distance from the nickel ion to its nearest neighbours, we have calculated the FT curve and fitted it to the FT one obtained from the treatment of the experimental EXAFS spectrum for the heated sample. This theoretical consideration was carried out using the standard program packet UWXAFS3.0 [12-13]. The initial distances Ni-Atom and their correction values obtained from the adjustment carried out with the help of the program FEFFIT5.0 from the UWXAFS3.0 are given in Table 2. The comparison of the theoretical and experimental FT is shown in Fig.2.

O	2.44	0.07
O	2.52	0.07
Mo (in tetrahedra)	2.75	0.21
O	2.83	-0.01
O	2.95	-0.01
Mo (in tetrahedra)	2.99	0.21
O	3.02	-0.16
O	3.21	-0.16
O	3.26	-0.16
Mo (in octahedra)	3.34	0.11
O	3.34	-0.16
O	3.36	-0.16
O	3.39	-0.16
O	3.45	0.10
Mo (in octahedra)	3.52	0.10
Mo (in octahedra)	3.54	0.10
O	3.57	0.01
Mo (in tetrahedra)	3.74	0.02
O	3.81	0.02
O	4.09	0.02

It can be concluded from Table 2 and Fig.3 that the assumed structure is satisfactory in reproducing the experimental curves in the region up to ~4 A. On the other hand, the values of the necessary corrections of these distances suggest that the real structure is close to the distorted

B) XANES analysis

Beside the analysis of the possible distances in the model, we have attempted to reveal, with the help of theoretical calculations, the effect of the geometry of molybdenum atom surroundings on the shape of the XANES curve near the K-edge of molybdenum absorption. The calculations were carried out for oxygen octahedron with molybdenum atom shifted from the centre of the octahedron by 0.4 A and less. Calculations were carried out also for a fragment of the octahedron including one edge and molybdenum atom. The calculations were carried out in Xα approximation in the framework of the method of multiple scattered waves (MS-method) following the program of Ruzankin S.F. [31]. Octahedron was modelled with the clusters $(NiO6)^{-10}$ and $(NiO6)^{0}$. Cluster charge was placed traditionally on the outer sphere which touched inner oxygen spheres. Overlapping of the spheres of oxygen centres and molybdenum was not larger than 6%. The results of the calculation revealed more close fit to the experimental curve (Fig.3) for the neutral cluster $(NiO6)^{0}$. This result is represented in Fig.4. A clearly marked shoulder in front of the absorption threshold was observed for the cluster $(NiO6)^{-10}$ with the traditional choice of the electron charge on the outscribed sphere of the cluster. This discrepancy between the theory and experiment is due to the inadequate choice of boundary conditions for the given fragment of NiO structure. Distinct corrections to O- and Ni- potentials from the ion lattice as a whole should be taken into account for this structure (Madelung's corrections). Without taking them into account, the high density of electron levels in the continuous spectrum beyond the absorption threshold is excessively shifted in the charged cluster to the bonded levels, thus causing the appearance of a marked shoulder before the absorption threshold. The choice of neutral cluster means that we artificially turn down the over-estimation of the potential inside the outer sphere, thus compensating the excessive shift of the levels. Absorption peak close to the K-threshold of nickel includes, due to the cluster symmetry, three equal contributions for three mutually perpendicular photon polarizations. Hence, the removal

Therefore, the decrease of the peak amplitude beyond the k-edge of nickel must be even more vividly expressed.

CONCLUSION

In general, to our opinion, we have every reason to believe that the first stage of the synthesis of high-temperature phase of nickel molybdate by the reaction $NiO+\alpha\text{-}MoO_3 \rightarrow \beta\text{-}NiOMoO_4$ leads to an intermediate phase different from the final product $\beta\text{-}NiOMoO_4$. In other words, the reaction proceeds without the formation of the layer of final product growing further across the whole region of the initial mixture. It is possible that initially NiO is dissolved in a modification of molybdenum oxide formed at the surface of $\alpha\text{-}MoO_3$ when heated above 600^0C. This could explain the observed high rate of the reaction. Our assumption on the possibility for the formation of the deformed structure of the phase $\gamma\text{-}Mo_4O_{11}$ is not in contradiction with the experimental data. Starting from this assumption, we can closely describe frr curve of our EXAFS experiment on Ni, give a qualitative explanation of the observed changes in the XANES spectrum beyond the K-edge of nickel absorption, as well as the reaction rate and its qualitative change. The work [32] should be noted dealing with the experimental study of the possibility for one of the oxides to be dissolved in the other through their common bounder. It is stressed in this work that this mechanism involving dissolution is able to provide substantially higher reaction rate than that given by the traditional diffusion mechanism.

The transformation of $\alpha\text{-}MoO_3$ into $\gamma\text{-}Mo_4O_{11}$ is accompanied by the release of oxygen: $4MoO_3 \rightarrow Mo_4O_{11}+O$. In the temperature range of the synthesis considered above, a strong adsorption of oxygen was observed on the surface NiO layer at large depth. A substantial number of nickel ions passing into the trivalent state is the reason [33]. This mechanism of absorbing the

concerning the possible mechanism of the reaction. This mechanism should be cleared in further experiments.

We thank the Russian Foundation of basic research (No.93-03-4235) and the International Science Foundation (Soros, No.6946-0925) for the financial support .

References

1. F. Di Reno, C.Mazzocchia.Reaction of Solids., **6**,145 (1988)

2. A.A. Slinkin, T.N. Kucherova, G. A. Ashavskaya and V.D. Nissenbaum. Kinetika i Kataliz (Russ.), **25**, N2, 431 (1984)

3. L.P. Plyasova, I.Yu. Ivanchenko, M.M. Andrushkevich et.al. Kinetika i Kataliz (Russ.), **14**, N4, 1010 (1973)

4. M Gleiser, W.L. Larsen, R.S. Speiser , and J.W. Spetnak. ASTM, **171**, , 65 (1955)

5. E.V. Tkachenko, V.M. Zuravlev. Zurnal Pricladnoi Himii (Russ.), **46**(10), 2129 (1973)

6. F. W. Kutzler, C.R. Natoli, D.K. Misemer, and et al. J.Chem.Phys., **73**, 3274 (1980)

7. C. R. Natoli. EXAFS and Near Edge Structure III, eds. K. Hodgson et. al. (Springer, Berlin, 1984), p.38

8. B.K. Teo. EXAFS. Basic Principles and Data Analysis, Inorganic Chemestry Consepts. **9**, (Springer, Berlin Heidelberg 1986)

9. D.C. Koningsberger, R. Prins (eds). Principles, Applications, Techniques of EXAFS, SEXAFS and XANES (Wiley, New York 1988)

10. J.J. Rehr. Physica , B**158,** 1 (1989)

11. V.A. Chernov, I.B. Drobyazko, S.G. Nikitenko. SSRC Activity Report-1990. INP, Novosibirsk, p.114-115, (1991)

15. D.E. Sayers, E.A. Stern, and F.W. Lytle. Phys. Rev. Lett., **27**, (1971) 1204

16. S.C. Abrahams, J.M. Reddy. J.Chem. Phys., **43**, 2533 (1965)

17. L. Kihlborg. Acta Chem. Scand., **13**, 954 (1959)

18. G. Swensson, L. Kihlborg. Reactivity of Solids, **3**, 33 (1987)

19. A. Magneli. Acta Chem.Scand., **2**, 861 (1948)

20. L. Kihlborg. Ark. Kemi, **21**, 471 (1963)

21. M. Ghedira, H. Vincent, M. Marezio and et.al. J.Sol. State Chem., **56**, 66 (1985)

22. A. V. Bessergenev, B.P. Tolochko. NIM, **A356**, 160 (1995)

23. K. Binder (ed.). Monte Carlo Methods in Statistical Physics. (Springer-Verlag, Berlin, Heidelberg, New-York, 1979)

24. L.V. Woodcock, C.A. Angell, P. Cheeseman. J.Chem.Phys., **65**, 1565 (1976)

25. S.K. Mitra, M. Amini, D. Finckam and R.W. Hockney. Philosophical Magazine, B**43**, 365 (1981)

26. G.V. Samsonov (ed.). Fiziko-himicheskie svoistva okislov. (Moskow,"Metalurgiya", 472 p., 1978)

27. S. Tanaka. J.Phys.Soc.Jap., **62**, 2112 (1993)

28. E.M. McCarton,J.C. Calabrese: Jour.Sol. Stat.Chem., **91**, 121 (1961)

29. G.W. Smith, J.A. Ibers. Acta Cryst.,**19**, 269 (1965)

30. G.W. Smith. Acta Cryst.,**15**, 1054 (1962)

31. S.F. Ruzankin.Zurnal Strukturnoi Himii. (Russ.), **20**, 953 (1972)

32. J.Haber. Pure&Appl. Chem., **56**, 1663 (1984)

33. S.F. Ruzankin. Thesis. (Institute of Catalysis, 630090 Novosibirsk, Russian Federation. 1982)

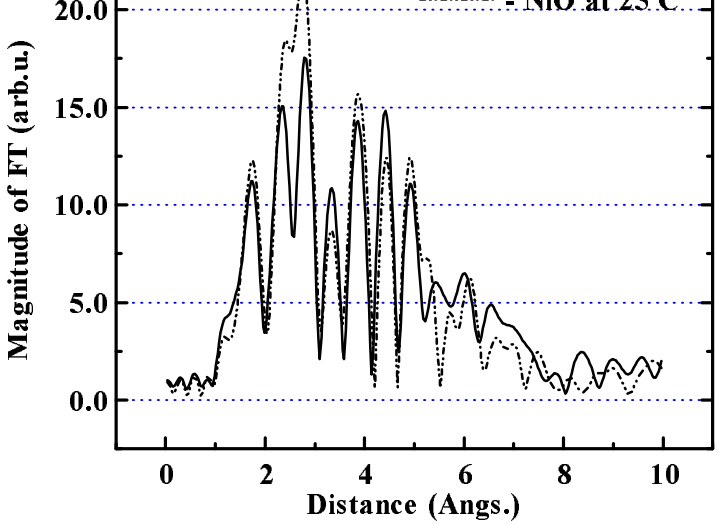

Figure 1.
Magnitude of the Fourier transformation of $k^3\chi(k)$ in the range 2.5-12.5(1/A) for Ni K-EXAFS

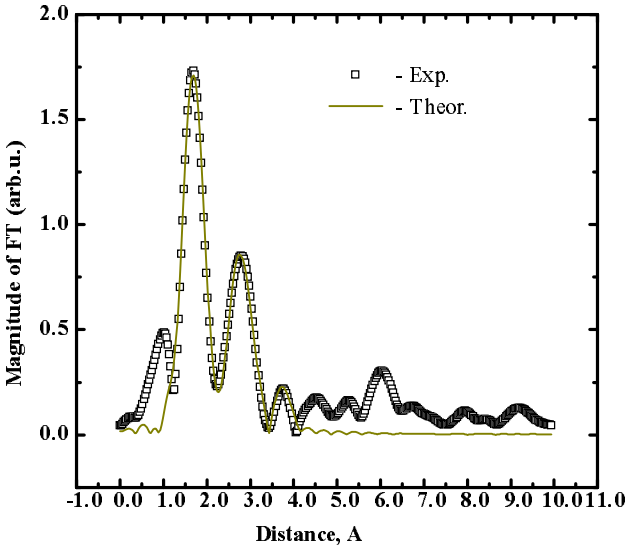

Figure 2.
Fourier transforms of Ni K-EXAFS for the product of the reaction of the mixture 0.1 NiO+1.0 MoO_3 after the heating over 600 C.

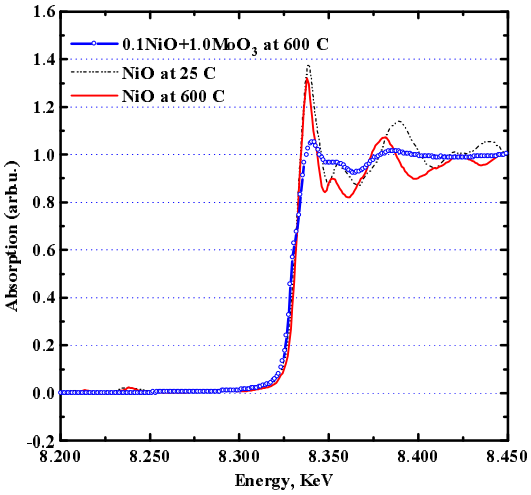

Figure 3.
Experimental XANES spectrum at K-edge of Ni atom.

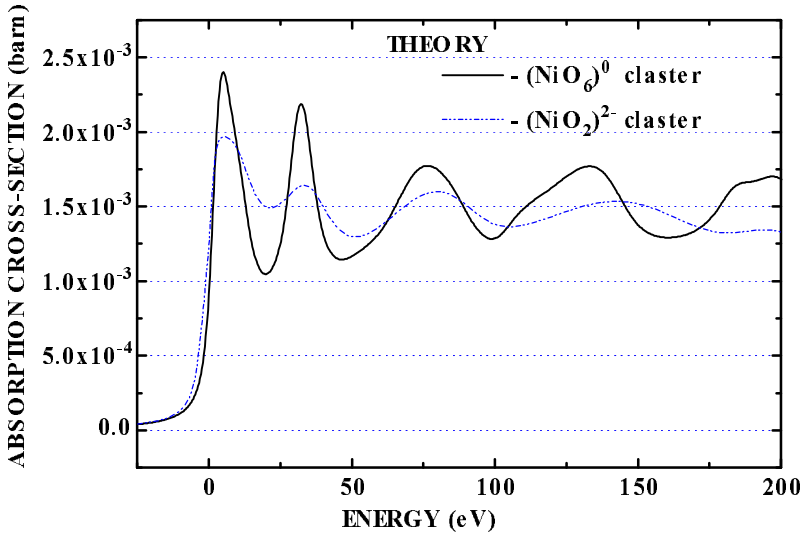

Figure 4.
Theoretical simulation of Ni K-XANES spectra for two different oxigen surroundings of Ni atom.